

Article

Autonomous Process Execution Control Algorithms of Solid Intelligent Backfilling Technology: Development and Numerical Testing

Tingcheng Zong^{1,2} , Fengming Li^{1,2}, Qiang Zhang^{1,2,*} , Zhongliang Sun³ and Haonan Lv^{1,2}

¹ School of Mines, China University of Mining & Technology, Xuzhou 221116, China; ts21020078a31@cumt.edu.cn (T.Z.); lifengming8005@163.com (F.L.); ts22020048a31@cumt.edu.cn (H.L.)

² State Key Laboratory of Coal Resources and Safe Mining, China University of Mining & Technology, Xuzhou 221116, China

³ Chengdu Sense Time Technology Company Limited, Chengdu 610213, China; 18339167680@163.com

* Correspondence: leafkky@163.com

Abstract: This paper analyzes the typical technical problems arising from dumping and tamping collision interferences in the working faces of conventional mechanized solid backfilling mining (SBM). Additionally, the technical and consecutive characteristics of the solid intelligent backfilling (SIB) method, the execution device, and the corresponding process categories of the SIB process are analyzed. A design for an SIB process flow is presented. Critical algorithms, including automatic recognition and optimization planning based on the cost function and laying the algorithm foundation, are proposed to develop a backfilling process control system. A joint simulation test system is built on a MATLAB/Simulink simulation toolkit (MSST) to simulate and test the optimized algorithms. The results show that the optimized algorithm can realize the automatic optimization planning and automatic interference-recognition adjustment of the backfilling process under actual engineering conditions. In conclusion, this paper analyzes typical technical problems in the conventional backfilling process, designs the SIB process flow, and develops key algorithms to achieve the automatic control of the backfilling process.

Keywords: solid intelligent backfilling; joint simulation; interference recognition



Citation: Zong, T.; Li, F.; Zhang, Q.; Sun, Z.; Lv, H. Autonomous Process Execution Control Algorithms of Solid Intelligent Backfilling Technology: Development and Numerical Testing. *Appl. Sci.* **2023**, *13*, 11704. <https://doi.org/10.3390/app132111704>

Academic Editors: Jianhang Chen, Krzysztof Skrzypkowski, René Gómez, Fhathuwani Sengani, Derek B. Apel and Faham Tahmasebinia

Received: 19 September 2023

Revised: 19 October 2023

Accepted: 20 October 2023

Published: 26 October 2023



Copyright: © 2023 by the authors. Licensee MDPI, Basel, Switzerland. This article is an open access article distributed under the terms and conditions of the Creative Commons Attribution (CC BY) license (<https://creativecommons.org/licenses/by/4.0/>).

1. Introduction

With the state's active promotion of intelligent coal mine construction [1,2] and the development of intelligent mines [3,4], the intelligent advancement of backfilling mining technology was also in full swing [5,6], and intelligence was the prevalent direction of future backfilling mining development.

The existing backfilling methods, such as tailings and cemented backfilling, based on industrial pumps and the pipeline transportation of cementitious materials, achieved a significant development in intelligent research and initially achieved intelligent control of the backfilling material, key parameters, and core processes [7,8]. However, the SBM method was based on the collaborative control of backfilling hydraulic support and a perforated bottom discharge scraper conveyor, and the difficulty lay in the high number of key parameters and intricate core procedure. Despite the application of electrohydraulic control technology in mechanical devices, full autonomy in the mining and backfilling processes was yet to be achieved. Consequently, intelligent research currently mainly focuses on device and process improvements, and the degree of its intelligence is gradually increasing with the development of technology.

In the research of intelligent mining's internal logic and operation mode, the research team of Wang et al. [9–11] designed a set of coal mine top-level system frameworks based on integrating intelligent management and control. Huang [12] constructed a logical

architecture centered on the “sensing, decision-making, execution and operation and maintenance” quadrants that could preliminarily realize the demand for intelligent and automatic mining. In the research on simulating intelligent mining devices, Liu et al. [13] proposed a method for establishing a digital twin model of equipment at a fully mechanized mining face. The study also conducted a simulation analysis of the fully mechanized mining process. Wang et al. [14] designed a virtual simulation system for solid backfilling hydraulic support (SBHS) based on Unity3D. The system utilized Unity3D to simulate the motion of the support. Yuan et al. [15] used MATLAB software (<https://ww2.mathworks.cn/en/products/matlab.html> (accessed on 10 October 2023)) to perform a kinematic simulation of a shielded hydraulic support. In terms of hydraulic support control algorithm development and testing, Tian et al. [16] combined BP neural network algorithms with PID control algorithms to achieve an online adjustment of PID parameters, improving the response speed and control accuracy of the hydraulic cylinders. Meng et al. [17] designed and built an emulsion/pure-water hydraulic cylinder precision push experiment platform that could complete eccentric loads, lateral loads, and other experiments on hydraulic cylinders, providing an experimental platform for the precise control of hydraulic cylinders and the coordinated control of hydraulic cylinder clusters.

The abovementioned literature mainly focuses on the automation and intelligence of fully mechanized mining equipment, while the research on the automation and intelligence of SBM technology is still limited and needs further investigation.

This paper analyzes the key links of the conventional mechanized backfilling process, clarifies the process organization requirements of the SIB working face, and designs the autonomous execution process of the coal mine SIB process flow. Based on the motion and positional constraint relationships between hydraulic support mechanisms, it develops algorithms for machine interference identification and tamping path planning to design an SIB process flow. It builds an SIB model simulation testing system to test and preliminarily validate the reliability of the algorithms.

2. Design for Solid Intelligent Backfilling Mining Process

2.1. Issues in the Execution of Dumping and Tamping Process

Backfilling technology can be divided into two stages: dumping and tamping. Firstly, the working face is filled to complete the front part of the coal cutting. The coal scraper conveyor is then pushed, followed by moving the frame and pushing the back part of the perforated bottom discharge scraper conveyor. The working face is filled straight at this point, and the backfilling technology can be executed. There are two typical kinds of pose interferences in the process [18]; one is dumping interference, which occurs when the tamping device is buried during the unloading of backfilling material from the middle slot of an open skylight in the dumping process, as shown in Figure 1.

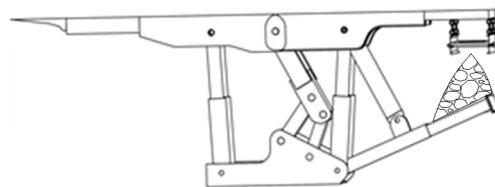


Figure 1. Dumping process interference.

The other one is collision interference, where the tamping device collides with the perforated bottom discharge scraper conveyor during the tamping process, as shown in Figure 2.

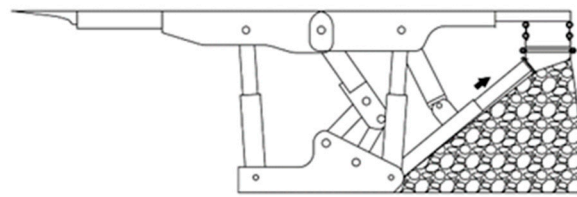


Figure 2. Tamping process interference.

2.2. The Solution for the Interference of Dumping and Tamping Processes

From the abovementioned analysis, it is evident that achieving the automatic control of fully mechanized coal mining solid backfilling technology is challenging due to the problems of dumping and collision interferences. Therefore, there is an urgent need to develop SIB technology with interference prediction and the automatic adjustment of the mechanism’s movement. Before performing the tamping process, it must be ensured that there is a suitable dumping clearance distance between the tamping device of the SBHS and the perforated bottom discharge scraper conveyor to ensure that the backfilling materials fall into the backfilling space. During the tamping process, it must be ensured that the SBHS tamping device is properly positioned concerning the perforated bottom discharge scraper conveyor during the movement of the tamping device. Therefore, it is essential to develop an “interference-recognition algorithm” [19,20] to achieve the abovementioned function. By analyzing the relationship between the dumping and tamping processes, an SIB process flow without human intervention was designed, as shown in Figure 3.

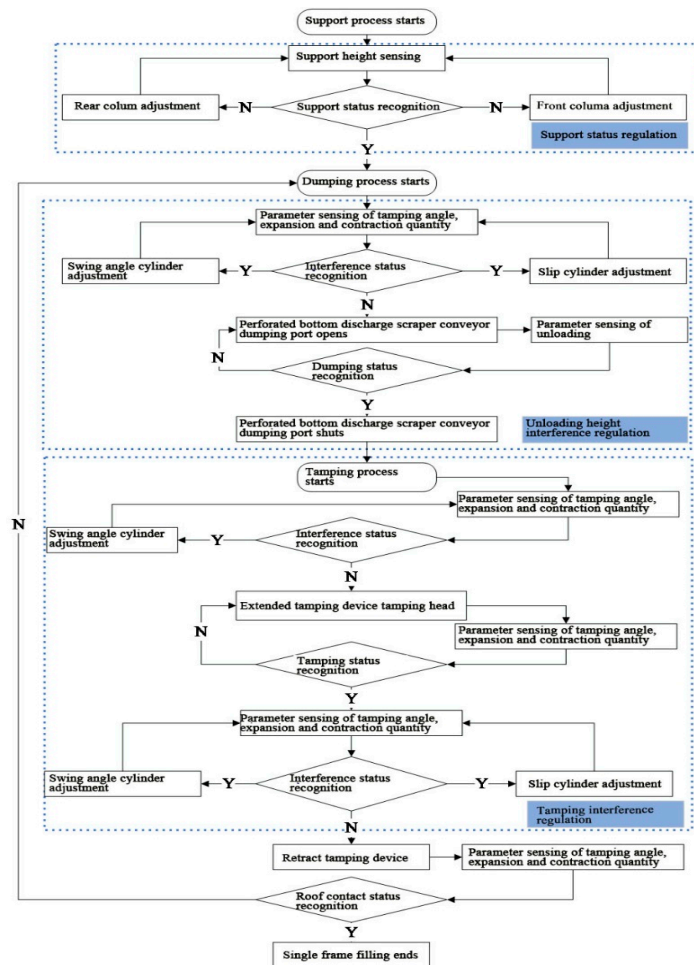


Figure 3. Solid intelligent backfilling process flow.

3. Interference Automatic Recognition and Tamping Path Planning

3.1. Interference Criticality Solving and Interference Automatic-Recognition Method

The SBHS tamping device is a two-degree-of-freedom structure [21], a rotating pair between the base and tamping device, and a moving pair between the primary and secondary tamping devices. A coordinate system was established to obtain the transformation relationship between the tamping device's head coordinates, tamping angle, and tamping path, as shown in Figure 4.

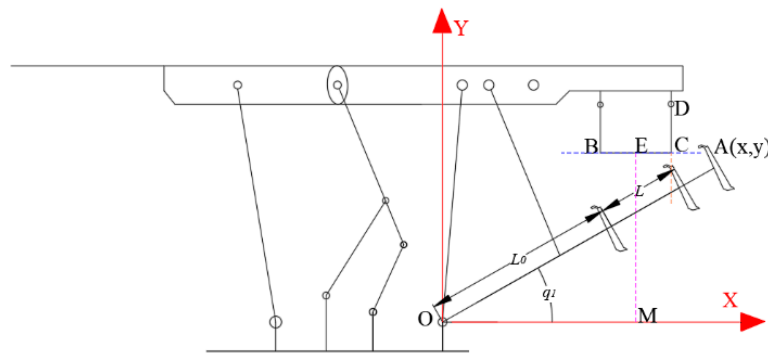


Figure 4. Interference critical analysis.

In Figure 4, BC and DC represent the bottom and rear boundaries of the perforated bottom discharge scraper conveyor, respectively; EM is the centerline of the dumping port of the perforated bottom discharge scraper conveyor [22,23]; L_0 is the unextruded length of the tamping device, mm; L is the tapping path, mm; q_1 is the tamping angle, °; $A(x,y)$ is the tamping head path function; x is the abscissa of the tamping head; y is the ordinate of the tamping head.

The kinematic equation establishment of the tamping device is as follows:

$$\begin{cases} x = L \cdot \cos(q_1) \\ y = L \cdot \sin(q_1) \\ L = L + L_0 \end{cases} \quad (1)$$

It is evident that to prevent any dumping interference in the dumping process, the tamping head coordinate must be positioned to the left of the EM straight-line portion before commencing the dumping. Therefore, the left side of the EM straight-line portion can be defined as the dumping non-interference area.

Similarly, during the execution of the tamping process, to prevent the collision interference between the tamping device and the bottom of the perforated bottom discharge scraper conveyor when the tamping device extends, it is only necessary to ensure that the tamping head coordinate is beneath the BC straight-line portion. When retracting the tamping device, it is necessary to ensure that the tamping head ordinate is smaller than the BC straight-line ordinate to avoid collision interference between the tamping device and the rear side of the multi-space perforated bottom discharge scraper conveyor, especially when the tamping head abscissa is higher than or close to the CD straight-line abscissa. For this reason, the area where the BC straight line rotates around point C to CD can be defined as the tamping non-interference area. Based on the abovementioned principles, an SIB process interference automatic recognition and regulation algorithm was designed, as shown in Figure 5.

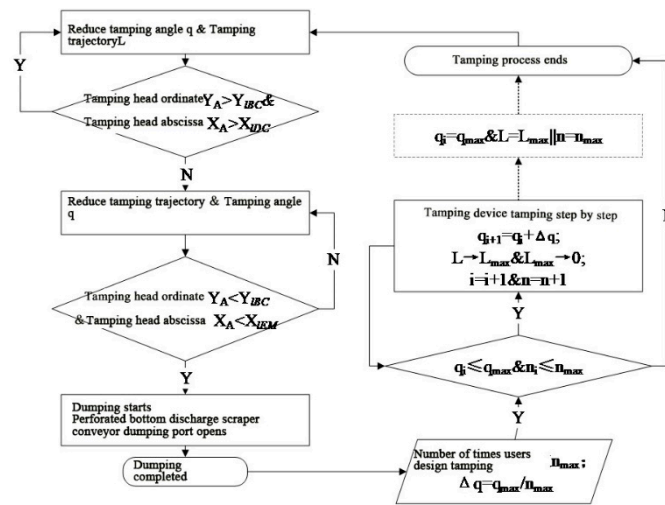


Figure 5. Automatic recognition and regulation algorithm of SIB process interference.

In Figure 5, L is the tamping path, mm; q is the tapping angle, °; Y_A is the ordinate value of the tamping head; X_A is the abscissa value of the tamping head; Y_{BC} is the ordinate value of the BC straight-line portion; X_{DC} is the abscissa value of the straight-line DC; X_{EM} is the abscissa value of the EM straight-line portion; Δq is the increment of the cyclic tamping angle adjustment, °; L_{max} is the maximum tamping path, mm; n_{max} is the maximum number of cycles required for user-defined and designed tamping processes; and q_i is the tamping angle of the i -th tamping, °.

The left part of Figure 5 displays the automatic recognition and regulation algorithm of the dumping process, while the right part shows the automatic recognition and regulation algorithm of the tamping process. In the SIB process, the dumping and tamping processes form a loop.

In addition, it is necessary to calculate the conversion relationship between the tamping head coordinate $A(x,y)$, tamping angle q_1 , and tamping path L for the tamping device, which mainly involves a swing angle cylinder and tamping cylinder, and where the driving parameters are the tamping angle and tamping path, as shown below:

$$\begin{cases} q_1 = -2 \cdot \arctan\left(\frac{x - \sqrt{x^2 + y^2}}{y}\right) \\ L_0 = \sqrt{x^2 + y^2} - L \end{cases} \quad (2)$$

3.2. Automatic Control of the Tamping Device Hydraulic Cylinder

(1) Construction of the hydraulic drive physical model for the tamping device.

For example, a hydraulic drive physical model was established for the tamping device cylinder. As the main driving component, the hydraulic cylinder mainly involved hydraulic pressure F_y and its corresponding hydraulic pump station, relating to hydraulic pressure P . The hydraulic drive model ensured a stable hydraulic pressure provided by the hydraulic pump station and controlled the tamping angle and path, as well as the stability of its angular and linear velocities, through the internal oil pressure F_y of the cylinder. The analysis process is as follows:

$$F_y = m_y a_y + B v_y \quad (3)$$

where B is the damping coefficient; v_y is the velocity of the cylinder motion; a_y is the cylinder motion acceleration; m_y is the payload quality of the cylinder; and F_y is the internal liquid pressure of the cylinder.

$$\begin{cases} \dot{x}_1 = a_y \\ x_1 = v_y \\ \dot{x}_2 = x_1 \\ F_y = U \end{cases} \quad (4)$$

Therefore:

$$U = m\dot{x} + Bx \tag{5}$$

The equivalent equation has the following form:

$$\begin{aligned} \dot{x}_1 &= -\frac{B}{m}x_1 + \frac{U}{m} \\ \dot{x}_2 &= x_1 \end{aligned} \tag{6}$$

where $x_1, x_2,$ and U are the conversion variables.

(2) Algorithm for automatic control of hydraulic cylinder position and motion.

To guarantee the stable and efficient navigation of the tamping device past obstacles towards its desired position, we used the common one (PID) control algorithm to build a PID closed-loop negative feedback controller for the position/motion control of the hydraulic cylinder, and the PID algorithm contained proportional, integral, and derivative parts. In the real control process, achieving the anticipated control effect involved continuous adjustments to the ratio coefficient K_p , integral time constant K_i , and differential time constant K_d parameters. The control principle diagram is shown in Figure 6 [24].

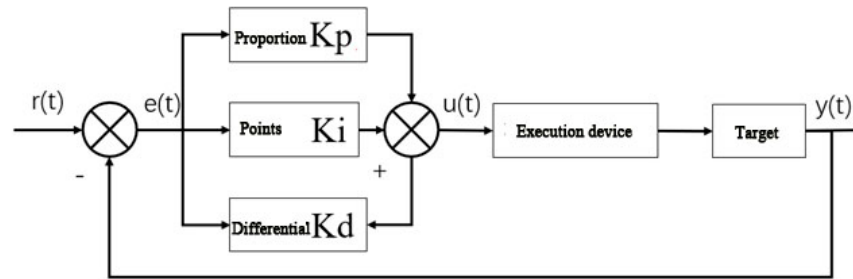


Figure 6. PID control system schematic diagram.

In Figure 6, $e(t)$ is the deviation between the input and output values, where $r(t)$ in $e(t) = y(t) - r(t)$ is the input value, $y(t)$ is the output value, t is the time interval between the start of the adjustment and the output of the current control quantity, and $y(t)$ is the input control signal at the moment when the PID starts adjusting. The adjustment process is a fixed value.

The hydraulic-cylinder-drive physical and PID control models were run using the MATLAB platform. Following a period of closed-loop control, the tamping angular velocity, angular acceleration, linear velocity, and linear acceleration of the tamping path of the tamping device all entered a stable state. The debugging results are shown in Figure 7.

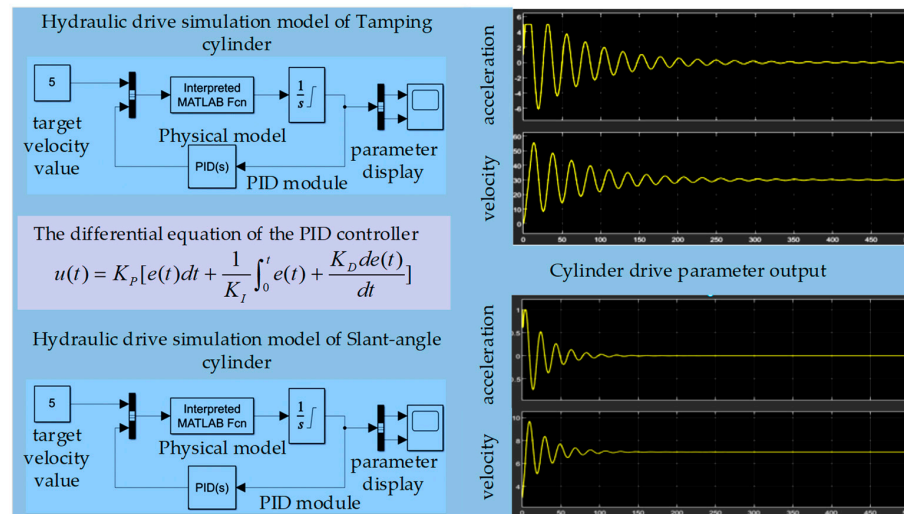


Figure 7. Hydraulic drive simulation model diagram.

3.3. Automatic Optimization Path Planning of the Tamping Device

During the movement of the tamping device, the tamping angle q_1 and tamping path L were functions of time t . By discretizing them, the point where the unit angle line intersected with the unit elongation line was determined as the movable position of the tamping device, and the path points within the movable range of the tamping device were obtained. The connection point between points was the movable path of the tamping device [25,26], forming the theoretical workspace lattice of the tamping device, as shown in Figure 8.

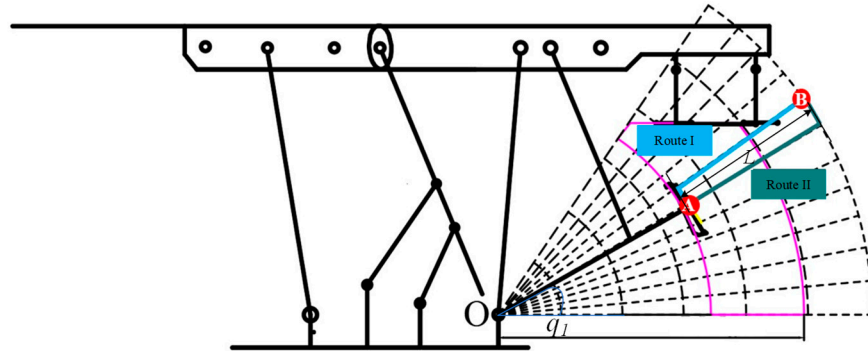


Figure 8. Movable path analysis diagram of the tamping device.

For a certain target location, the motion path of the tamping device included multiple paths. To achieve the automatic optimization planning of the tamping device path, the cost function was used to calculate the corresponding costs of multiple movable paths, and the optimal path selection was achieved by minimizing the cost. The cost function considers interference avoidance, angle adjustment, and elongation (path) adjustment.

$$F(i) = Z * \{w_q F(q) + w_L F(L)\} \tag{7}$$

where i is the alternative path label; $F(i)$ is the cost function; the Z value (0 or 1) indicates whether there are obstacles or not, respectively; $F(q)$ is the angle adjustment cost; $F(L)$ is the elongation (path) adjustment cost; w_q is the angle adjustment weight; and w_L is the path adjustment weight.

The value of Z was only 0 or 1, indicating whether there were obstacles or not. If there were obstacles, it was 0, indicating that the path cost was 0 and not selected. The weight was designed based on the actual impact of the working environment on the hydraulic adjustment. Due to the on-site data showing a higher cost of the angle adjustment, the angle adjustment weight exceeded the path adjustment weight.

For example, as shown in Figure 8, the tamping device has multiple paths to choose from, such as Paths I and II, from the current position A to the target position B in the movable paths set. From Equation (7), it is evident that both paths have the same costs as angle adjustments. Path I had a pose interference, $Z = 0$, and this path was discarded; Path II had no interference, $Z = 1$, and Path II was selected.

Based on the cost function principle, an automatic optimization planning of the tamping device motion path was achieved. Combined with the backfilling process interference automatic recognition and regulation algorithm previously constructed, as well as the control algorithm of the hydraulic cylinder, an intelligent control system of the backfilling operation movement was formed.

4. Establishment of the Simulation Test System and Design of Testing Methods

4.1. Design of the Simulation Test System Architecture

To guarantee the efficacy of simulation testing, the simulation test system was designed with three major functions: mechanical assembly and motion simulation, electrohydraulic

control system simulation, and process action automatic-execution algorithm simulation. The system architecture is shown in Figure 9.

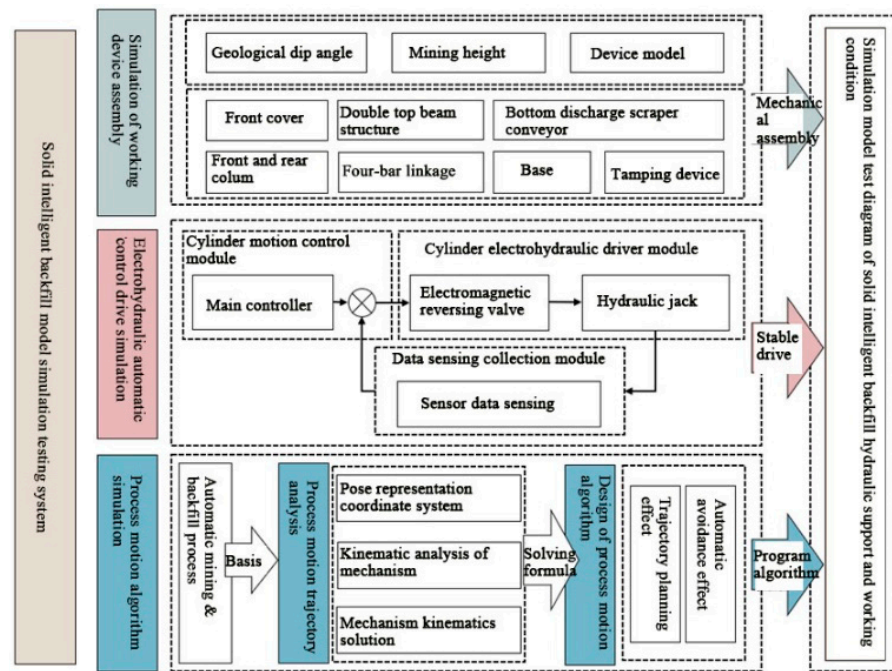


Figure 9. Architecture diagram of SIB process motion simulation testing system.

In Figure 9, the mechanical assembly and motion simulation function is achieved using SolidWorks to model, assemble, and provide a 3D motion simulation of the SBHS. It can perform a mechanical assembly and motion simulation of key mechanisms, which is the foundation of the entire simulation testing system. The simulation system of the hydraulic cylinder electrohydraulic control system was implemented through the MATLAB platform, which could analyze and simulate the driving process of the hydraulic cylinder, ensure the stability of the hydraulic cylinder speed, and ensure the effectiveness of the process action automatic-execution algorithm testing. The process action automatic-execution algorithm simulation function was implemented through the joint simulation of MSST and SolidWorks [27,28]. Based on the SIBPF, the process action automatic-execution algorithm was designed, mainly including the interference automatic-recognition and path automatic-planning algorithms.

4.2. Establishment of the Simulation Test System

(1) Three-dimensional model construction.

The SBHS model was assembled from key structures, such as a perforated bottom discharge scraper conveyor and tamping device, as shown in Figure 10.

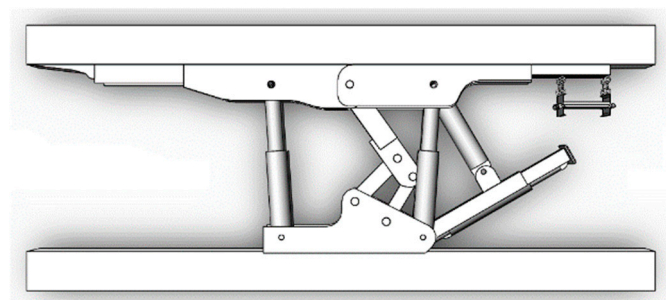


Figure 10. Assembly drawing of the support mechanical model.

The Simscape Multibody Link plugin can automatically convert the 3D geometric solid model established by SolidWorks into a SimMechanics model [29], as shown in Figure 11.

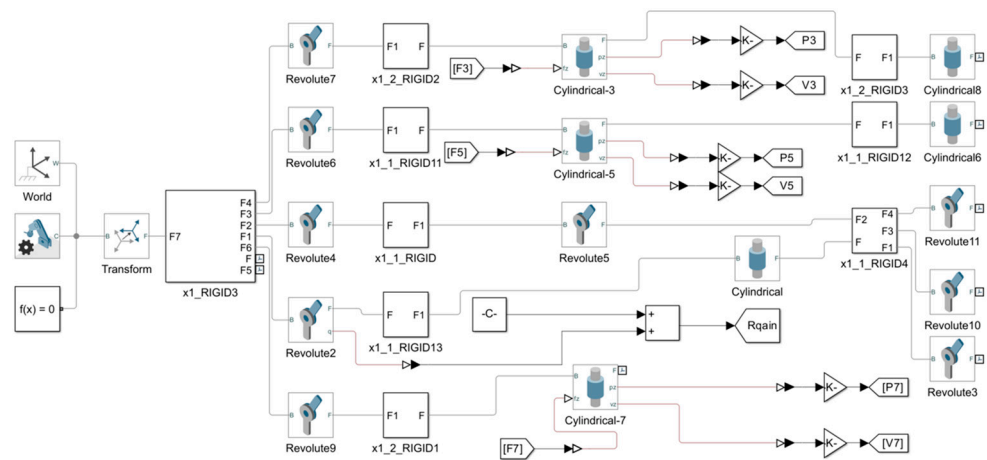


Figure 11. Backfilling hydraulic support SimMechanics model.

(2) Key parameter collection.

To achieve a simulation of the backfilling process, it was first necessary to implement the control of the backfilling hydraulic support model. Therefore, it was necessary to collect the paths of each hydraulic cylinder in the backfilling hydraulic support in real time. For example, the support process required obtaining the front and rear column paths to grasp the front top beam’s support height and inclination angle. Key parameters, such as the expansion and contraction quantities of the perforated bottom discharge scraper conveyor, tamping path, tamping angle, and tamping pressure must be obtained in both the unloading and tamping processes. Correspondingly, the distance, angle, and pressure sensors were used, and those sensors were set in the model to monitor the positions [30], as shown in Table 1.

Table 1. Monitoring parameter settings and sensor arrangement for the backfilling hydraulic support model.

No.	Parameter Type	Sensor Type	Installation Position
1	Front column path ΔL_f	Range sensor	Front-column hinge joint A
2	Rear column path ΔL_h	Range sensor	Rear-column hinge joint B
3	Front top-beam height H_B	Range sensor	Front top-beam hinge joint C
4	Expansion and contraction quantities of perforated bottom discharge scraper conveyor ΔL_s	Range sensor	Scraper and jack hinge joint D
5	Tamping pressure F_N	Pressure sensor	Tamping head junction E
6	Tamping path L_0	Range sensor	Tamping head junction F
7	Tamping angle q_1	Angle sensor	Tamping-device hinge joint G

The installation location and model’s data collected by the sensor on the model are illustrated in Figure 12.

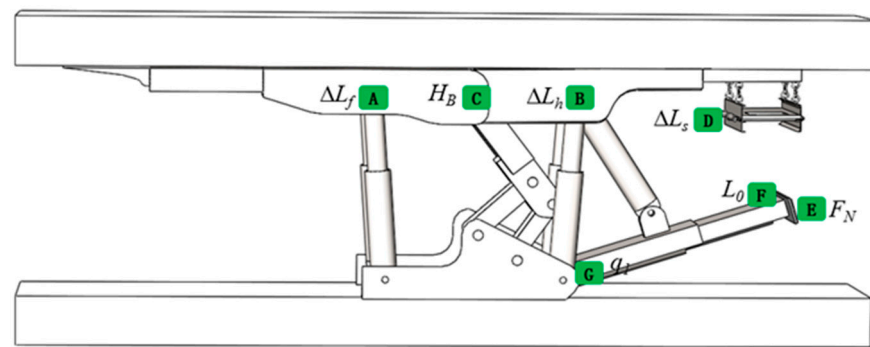


Figure 12. Installation design drawing of model sensor.

(3) Cylinder electrohydraulic drive function.

The expansion and contraction of each hydraulic cylinder in the backfilling hydraulic support were controlled by an electromagnetic directional valve. The electromagnetic directional valve belonged to a switch valve and its extension/retraction state corresponded to the extension and retraction states of the hydraulic cylinder. The opening time corresponded to a certain number of extension and retraction paths of the hydraulic cylinder. The reversing valve and corresponding cylinder settings in the model are shown in Figure 13.

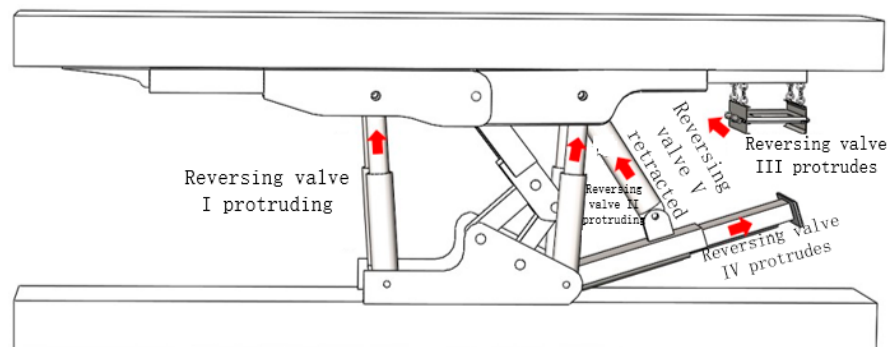


Figure 13. Model reversing-valve cylinder configuration design diagram.

Among them, the support process controlled the path of the front and rear columns by controlling the extension/contraction states of reversing valves I and II. The unloading process controlled the dumping cylinder of the perforated bottom discharge scraper conveyor by controlling the extension/contraction states of reversing valve III, thereby simulating the control of the unloading volume. The tamping process controlled the compaction and swing-angle cylinder paths by controlling the extension/contraction states of reversing valves IV and V, thereby achieving the control of the tamping head path, which was the main control object for the interference automatic-recognition and the path automatic-planning algorithms.

(4) Establishment of SolidWorks and (MSST) joint-simulation testing system.

The joint simulation testing system is shown in Figure 14. The key steps for the system setup are as follows:

(i) Build a PID hydraulic drive model for each hydraulic cylinder in the backfilling hydraulic support on the MSST and connect it to the motion joints in the SimMechanics model to serve as a controller for hydraulic cylinder actions.

(ii) Using the MSST, write the SIB process interference automatic recognition and regulation algorithm and the tamping path automatic-planning algorithm into the MATLAB-Function module and construct the process action automatic-execution algorithm module based on the SIBPF previously designed.

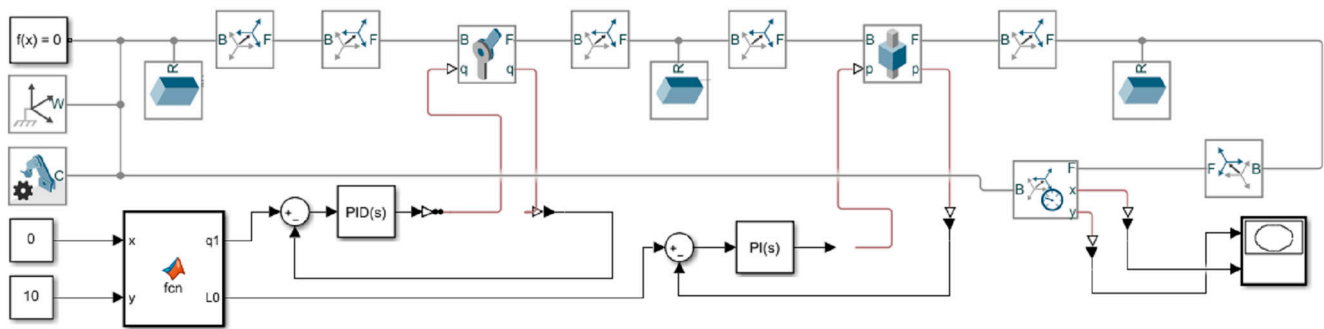


Figure 14. Joint-simulation testing system of SolidWorks and MATLAB/Simulink.

(iii) Use the constant module to set each hydraulic cylinder's target positions, i.e., operating parameters, in the backfilling hydraulic support. When executing the internal interference automatic-recognition and tamping path automatic-planning algorithms in the module, the tamping angle q_1 and tamping path L obtained from the algorithm will be transmitted to the PID control module of the hydraulic drive simulation model, thereby controlling the movement of the tamping device.

(iv) Finally, the coordinate transformation sensor was used to output the motion path data of the tamping device, and the process motion path of the tamping head in the absolute coordinate system was displayed in the SBHS model built by SolidWorks.

4.3. Design of the Simulation Testing Plan and Process Simulation

Based on the simulation testing system previously established, different simulation testing schemes could be achieved by setting and adjusting the operating parameters, such as the support inclination angle and height; the initial states of driving parameters, such as the tamping angle, tamping path, and column path; as well as the target position of the tamping device motion.

This study simulated the support, dumping, and tamping processes using the column, swing-angle cylinder, and tamping cylinder path as the driving parameters. Before the start of the support process, the initial value of the support height was 2980 mm, the target position was 3550 mm, and the simulation path was A_1 - A_2 . Before starting the tamping process, the initial value of the tamping angle was 9° and the initial value of the tamping path was 600 mm. By setting the target position points of the tamping process to C_2 and C_5 , the tamping device was controlled by the interface automatic-recognition and tamping path automatic-planning algorithm modules, also known as the process action automatic-execution algorithm module, and the simulation path was C_1 - C_2 - C_3 - C_4 - C_5 . After the tamping process was completed, resetting the tamping device to the initial position before the dumping process started to prepare for the next dumping and tamping cycles was necessary. Before the dumping process started, the initial position of the tamping device was C_5 , the target position point of the tamping device in the dumping process was C_8 , and the simulation path was C_5 - C_6 - C_7 - C_8 . The abovementioned simulation results are shown in Figure 15.

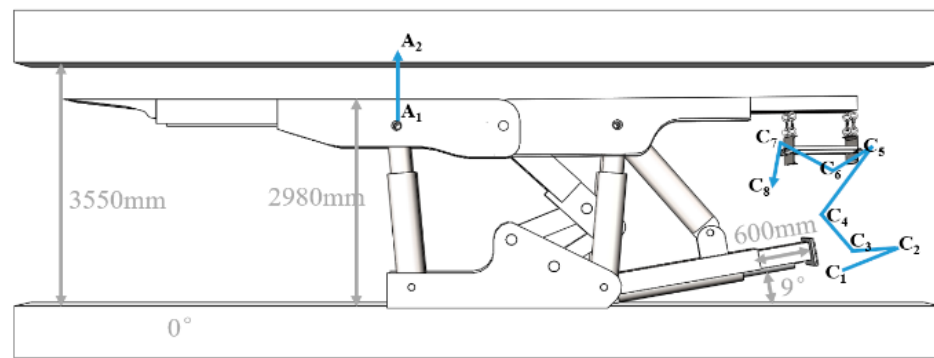


Figure 15. Simulation model test diagram of the SIB hydraulic support.

From Figure 15, it can be seen that the motion path of the tamping device does not reach the optimal path. During the movement process, there was a collision interference with the perforated bottom discharge scraper conveyor. For the C₅-C₆ and C₆-C₈ segments, the optimal action sequence should first reduce the tamping path and then increase the tamping angle to avoid collision interference. As shown in Figure 5, when the tamping angle reaches the maximum value, it needs to be further increased to trigger the tamping end process, which initiates the dumping interference-recognition part. This process might cause instability in the tamping device motion, leading to interference. Therefore, it was necessary to improve the process action automatic-execution algorithm module. The optimization of the algorithm is shown in the dashed box in Figure 5. The tamping device tamping angle and tamping path reaching the maximum value were used as discriminant markers for the end of the tamping, thus avoiding the abovementioned problems.

5. Engineering Cases

5.1. Overview of the Working Face and Process of the Solid Intelligent Backfilling

The SIB mining face of a particular coal mine in Xingtai taken as the case study was located in the first level-2# coal seams mining area, with an average thickness of 4.4 m and an average inclination angle of 8° for the coal seams. The old top was gray–white fine sandstone with a thickness of 5–8.5 m, and the direct top was dark-gray sandy mudstone with a 1.49–6 m thickness. The direct floor was black siltstone with a thickness of 0.40–1 m and the old bottom was gray, medium-grained sandstone with a 3–4.83 m thickness. The working face coal seams had a stable thickness and simple structure. The coal seams had a strike of 92–131°, a dip of 2–41°, an inclination angle of 3–12°, and a hardness coefficient of 0.62.

By analyzing the key geological parameters, such as the average thickness of the SIB mining-face coal seams, the average inclination angle of the coal seams, the mining length, and the recoverable reserves of the abovementioned mine in Xingtai, the respective parameters of the SIB mining working face were used, as listed in Table 2.

Table 2. SIB mining working face parameters.

Working Face Name	Working Face Length/m	Mining Distance/m	Mining Height/m	Average Inclination Angle/°	Recoverable Reserves/10,000 t
1#	58	633	4.4	8	21.6
2#	58	880	4.6	12	31.5
3#	58	730	4.5	11	25.5

The SIB mining face of the case study coal mine had abandoned the comprehensive mechanized backfilling technology of operating SBM devices with the staff as the core for full mining-height tamping.

The SIB technology of this working face comprised a sensing process, recognition process, pose adjustment and support processes, unloading process, and tamping pro-

cess. The key SIB technology included operation movement, execution mechanism, and corresponding process categories, as shown in Table 3.

Table 3. Mining and backfilling process table for the SIB mining method.

No.	Device Name	Operation Movement	Execution Device	Process Category
1	Backfilling hydraulic support	Roof guard Moving frame, lifting frame Sensing of parameters, such as support height Pose interference recognition	Cylinder guard Cylinder bottom, column Sensing element Recognition module	Support process Support process Sensing process Recognition process
2	Tamping device	Tapping angle change Sensing of parameters, such as sampling angle Pose interference demodulation	Tamping cylinder Slant-angle cylinder Sensing element Tamping cylinder, slant-angle cylinder, etc.	Tamping process Tamping process Sensing process Pose adjustment process
3	Perforated bottom discharge conveyor	Material transportation Dumping port switch Body position slip Sensing parameters, such as dumping height Pose interference demodulation	Scraper chain Dumping cylinder Slip cylinder Sensing element Dumping cylinder, Slip cylinder	Unloading process Unloading process Unloading process Sensing process Pose adjustment process

After designing the SIB technology, various sensors were used to obtain the backfilling hydraulic support status and pose information. The optimized process action automatic-execution algorithm module controlled the execution of the support cyclone action. It controlled the electrohydraulic control system to execute the cylinder action without the need for coal-mining machine shutdown or human intervention, saving the continuation time of the cylinder action, reducing personnel, increasing efficiency, and ensuring a safe production.

5.2. Model Operating-Condition Parameter Setting and Simulation Testing Scheme Design

An SIB technology testing model was built based on the SIB model simulation testing system, combined with the mining geological conditions and filling equipment parameters of the SIB working face for the case-study coal mine. The pre- and post-improvement process action automatic-execution algorithm modules were used for the simulation testing to compare the improvement effect of the process action automatic-execution algorithm.

According to the test model design in Table 4, the SBHS's inclination angle was set at 8°, the mining height was set at 4400 mm, and the equipment model was a four-column backfilling hydraulic support. In the initial state, the device assembly simulation model had a sampling angle of 6°, a sampling path of 400 mm, and front and rear column paths of 620 mm were used as the carrier, while the front and rear columns, slant-angle cylinder, and tamping cylinder were used as the drivers. The A_1 – A_2 path of the support process and C_1 – C_2 – C_3 – C_4 – C_5 – C_6 – C_7 – C_8 – C_9 of the tamping process were run for the simulation testing, as shown in Figure 16.

Table 4. SIB working-face test model design information.

Design Object		Key Design Information		
Assembly design	Working environment	Inclination angle/°	Mining height/mm	Device model
		8	4400	Four-column type
Initial state		Tamping angle/°	Tamping path/mm	Column path/mm
		7	60	3000
Drive design	Drive cylinder	Front and rear columns		Slant-angle cylinder, tamping cylinder
	Key parameters	Front and rear column paths		Tamping angle, tamping path
Process plan	Process category	Support process		Tamping process
	Motion path	A_1-A_2		$C_1-C_2-C_3-C_4-C_5-C_6-C_7-C_8-C_9$

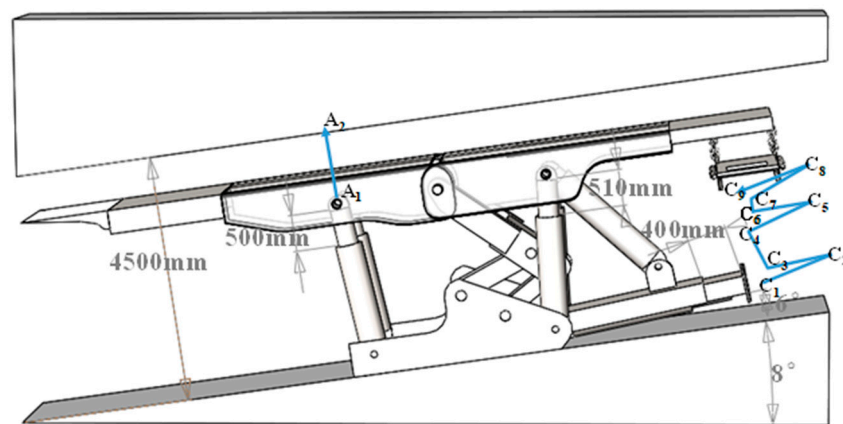


Figure 16. SIB process testing model diagram.

5.3. Quantitative Analysis of the Test Results

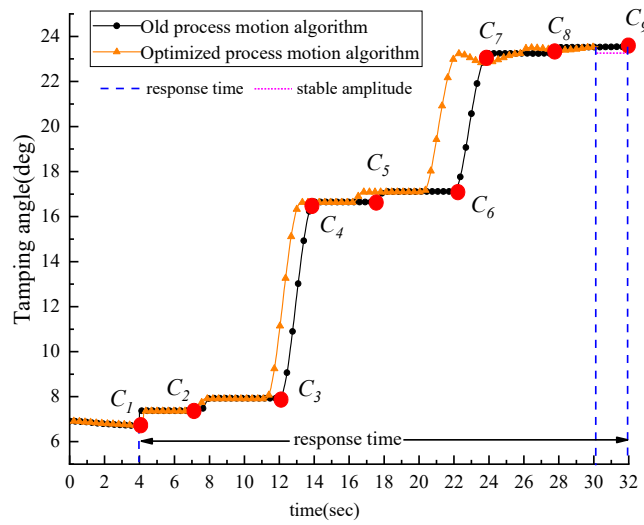
The motion path of the tamping device of the SBHS in the simulation testing model is shown in Figure 16. The model sensor module was used to output and analyze the path curve during the simulation process.

The variations of the tamping device of the SBHS tamping angle and path under the control of two algorithms during the process simulation are shown in Figure 17.

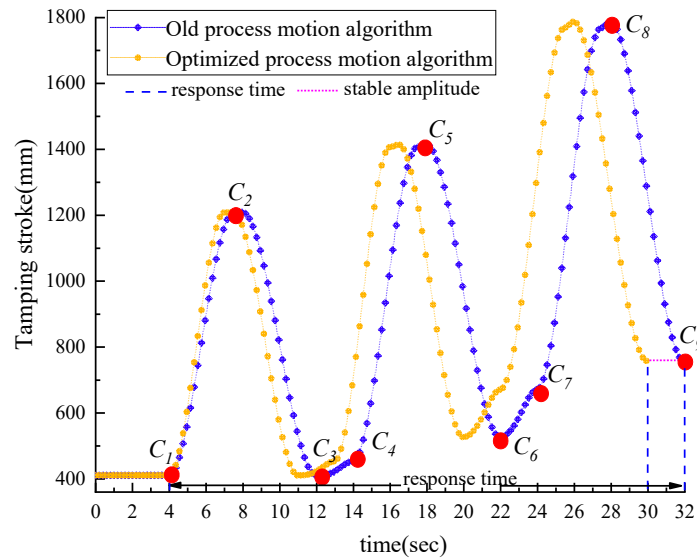
From Figure 17a,b, it can be seen that the response time of the old process action automatic-execution algorithm for controlling the tamping angle and tamping path is 32 s. The optimized process action automatic-execution algorithm for controlling the timing tamping angle and tamping path has a response time of 30 s, which improves the efficiency by 7%. In both cases, the tamping angle and path reach the target position C_1-C_9 with a small amplitude difference and do not result in pose interference.

The column path variations in the process simulation under the control of two algorithms are shown in Figure 18.

Figure 18 shows that, during the 2.0 s operation of the column, a pose interference g_1 occurs in the optimized process action automatic-execution algorithm. The optimized process action automatic-execution algorithm successfully conducts interference recognition s_1 and autonomously regulates b_1 . The regulation is successful at around 3.2 s, and the columns overlap with the ideal state to achieve automatic avoidance. It reaches the target position A_2 of the process in 3.5 s.



(a) Variation chart of tamping device tamping angle.



(b) Variation chart of tamping device tamping path.

Figure 17. Comparison of control effects of different algorithms on the tamping device.

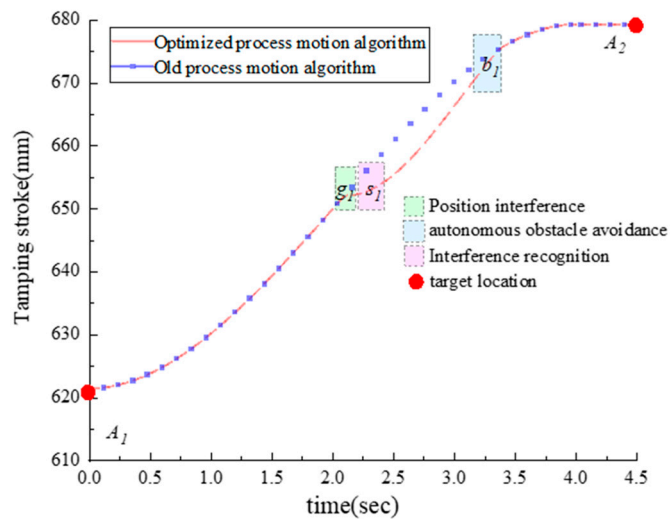


Figure 18. Comparison of control effects of different algorithms on the column.

The motion path of the tamping device under the control of two algorithms during the process simulation is shown in Figure 19.

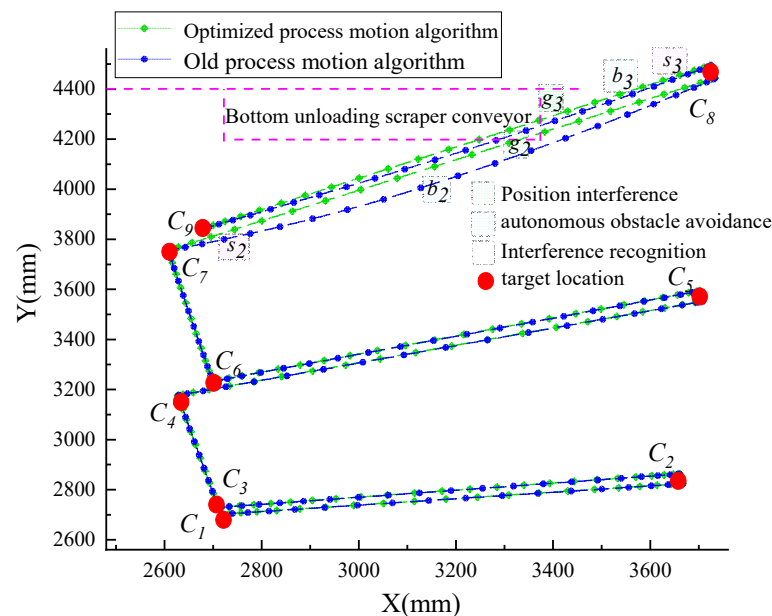


Figure 19. Motion path diagram under different algorithm controls.

Figure 19 shows no abnormalities in the C_1 – C_7 process. In C_7 – C_8 and C_8 – C_9 , the tamping device and the perforated bottom discharge scraper conveyor collide. The interference-recognition algorithm identifies s_2 and s_3 values, automatically avoiding b_2 and b_3 . However, automatic avoidance b_3 still has a slight collision interference due to the low-accuracy control.

6. Conclusions

(1) This study investigated the dumping interference and tamping collision interference problems in a conventional mechanical solid backfilling working face. It designed the SIB process flow to mitigate these problems, providing a theoretical basis for realizing the intelligent control of the solid backfilling process.

(2) Crucial algorithms were proposed for the automatic interference recognition and planning the motion path of the tamping mechanism in an SIB process, including the interference automatic-recognition algorithm and automatic optimization planning algorithm based on the cost function, laying the algorithm foundation for the development of a backfilling process control system.

(3) A joint-simulation test system was built on the MSST to run and validate the optimized algorithms. The results show that the optimized algorithm can efficiently realize the automatic optimization planning and automatic interference-recognition adjustment of the backfilling process under actual engineering conditions.

Author Contributions: Conceptualization and methodology, T.Z. and Q.Z.; software and validation, T.Z., F.L. and Z.S.; formal analysis, H.L.; investigation, F.L.; resources, Z.S.; data curation, H.L. and F.L.; writing—original draft preparation, T.Z.; writing—review and editing, Q.Z.; visualization, Q.Z.; supervision, Q.Z.; project administration, T.Z.; funding acquisition, Q.Z. All authors have read and agreed to the published version of the manuscript.

Funding: The work was supported by the National Natural Science Foundation of China (Grant No. 52174134), the Fundamental Research Funds for the Central Universities (Project No. 2021GJZPY12), Funded by the Graduate Innovation Program of China University of Mining and Technology (Project No.2023WLJCRCZL036), Funded by the Postgraduate Research & Practice Innovation Program of Jiangsu Province (Project No. KYCX23_2807).

Institutional Review Board Statement: Not applicable.

Informed Consent Statement: Not applicable.

Data Availability Statement: The data presented in this study are available on request from the corresponding author.

Conflicts of Interest: The authors declare no conflict of interest.

References

1. He, M.; Wang, Q.; Wu, Q. The future of mining: Thinking about the construction of intelligent 5G N00 mines. *China Coal* **2020**, *46*, 1–9.
2. Wang, G.; Zhao, G.; Ren, H. Analysis on the key core technologies of smart coal mine and intelligent mining. *J. Coal* **2019**, *44*, 34–41. [[CrossRef](#)]
3. Fan, J.; Li, C.; Yan, Z. The overall architecture and core scenarios of intelligent coal mines integrating 5G technology ecology. *J. Coal Sci.* **2020**, *45*, 1949–1958. [[CrossRef](#)]
4. Zhang, F.; Ge, S.; Li, C. Research summary on digital twin technology for smart mines. *Coal Sci. Technol.* **2020**, *7*, 168–176. [[CrossRef](#)]
5. Zhang, Q.; Zhang, J.; Wu, Z.; Chen, Y. Overview of Solid Backfilling Technology Based on Coal-Waste Underground Separation in China. *Sustainability* **2019**, *11*, 2118. [[CrossRef](#)]
6. Bo, L.; Yang, S.; Liu, Y.; Zhang, Z.; Wang, Y.; Wang, Y. Coal Mine Solid Waste Backfill Process in China: Current Status and Challenges. *Sustainability* **2023**, *15*, 13489. [[CrossRef](#)]
7. Hu, Y.; Li, K.; Zhang, B.; Han, B. Strength Investigation and Prediction of Superfine Tailings Cemented Paste Backfill Based on Experiments and Intelligent Methods. *Materials* **2023**, *16*, 3995. [[CrossRef](#)] [[PubMed](#)]
8. Tran, V.Q. Using Artificial Intelligence Approach for Investigating and Predicting Yield Stress of Cemented Paste Backfill. *Sustainability* **2023**, *15*, 2892. [[CrossRef](#)]
9. Wang, G.; Ren, H.; Zhao, G.; Du, Y. Digital model and giant system coupling technology system of smart coal mine. *J. China Coal Soc.* **2022**, *47*, 61–74. [[CrossRef](#)]
10. Wang, G.; Ren, H.; Pang, Y.; Zhang, X. Research and engineering progress of coal mine intelligent (primary stage) technology system. *Coal Sci. Technol.* **2020**, *48*, 1–27.
11. Wang, G.; Du, Y.; Ren, H.; Fan, J.; Wu, Q. Research and practice of top-level design of intelligent coal mines. *Chin. J. Coal* **2020**, *45*, 1909–1924. [[CrossRef](#)]
12. Huang, Z. Exploration and research on transformation from intelligent single machine equipment to intelligent synergy in coal mine. *Coal Sci. Technol.* **2021**, *49*, 169–175. [[CrossRef](#)]
13. Liu, Q.; Zhang, L.; Li, T.; Du, P. A three machine digital twin and collaborative modeling method for fully mechanized working face. *J. Mine Au-Tomation* **2023**, *49*, 47–55. [[CrossRef](#)]
14. Wang, Y.; Shi, Y.; Wang, Y.Y.; Qi, P.L.; Wang, H.Q. Full pose measurement and virtual simulation of solid filling hydraulic support. *J. Mine Autom.* **2022**, *48*, 81–89. [[CrossRef](#)]
15. Yuan, X.; Gao, F.; Lian, Z. Kinematics Simulation and Experiment Investigation of Shield Powered Support Based on MATLAB. *Chin. Hydraul. Pneum.* **2021**, *45*, 25–31. [[CrossRef](#)]
16. Tian, J.; Li, Y.; Zhang, L.; Liu, Z. Adaptive control of temporary support force based on PSO-BP neural network. *J. Mine Autom.* **2023**, *49*, 67–74. [[CrossRef](#)]
17. Meng, L.; Zhou, R.; Guo, Z. Design and research of hydraulic cylinder precise control test system. *Coal Sci. Technol.* **2023**, *51*, 237–245. [[CrossRef](#)]
18. Zong, T.; Zhang, Q.; Shi, P. Critical characterization of solid-filled hydraulic support mechanism interference and autonomous demodulation method. *Coal Sci. Technol.* **2023**, *51*, 260–270.
19. Yang, Y.; Wang, Y.; Zhang, Q.; Cheng, G. Mechanism of interference discrimination and adjustment in the mechanical independent compaction process of intelligent solid backfilling method. *J. Min. Saf. Eng.* **2022**, *39*, 921–929.
20. Zhang, Q.; Wang, Y.; Zhang, J.; Zhang, Z. Research on intelligent filling mining method for coal mine solids. *J. Coal* **2022**, *47*, 2546–2556.
21. Ren, H.; Li, S.S.; Li, X.; Fu, Z. Simulation analysis of the position and posture control of hydraulic support roof beam. *Ind. Min. Autom.* **2019**, *45*, 11–16.
22. Zhang, Q.; Liu, Y.; Zhang, J.; Zhang, H.; Yin, W.; Wang, H. Influencing factors and control methods of mechanism interference in the autonomous compaction process of solid intelligent filling. *J. Coal* **2022**, *47*, 1043–1054. [[CrossRef](#)]
23. Shi, P.; Zhang, J.; Yan, H.; Zhang, Y.; Zhang, Q. Evaluation of Operating Performance of Backfilling Hydraulic Support Using Six Hybrid Machine Learning Models. *Minerals* **2022**, *12*, 1388. [[CrossRef](#)]
24. Gao, B.; Li, F. Posture Control of Hydraulic Proportional Drive Robot Arm Based on Inclination Sensor. *Mach. Tool Hydraul.* **2023**, *51*, 38–44.
25. Fang, X.; Liang, M.; Li, S.; Zhang, L. Key technologies for multi-parameter accurate perception and safety decision-making in intelligent working face. *J. Coal Sci.* **2020**, *45*, 493–508. [[CrossRef](#)]

26. Yang, Q.; Qu, D.; Xu, F. Path planning for mobile robots based on motion prediction of obstacles. *Comput. Eng. Des.* **2021**, *42*, 182–188. [[CrossRef](#)]
27. Zhu, Y. Application of SolidWorks in hydraulic support design. *Coal Min. Mach.* **2013**, *34*, 237–239. [[CrossRef](#)]
28. Huang, N.-B.; Kang, H.J. Observer-based dynamic parameter identification for wheeled mobile robots. *Int. J. Precis. Eng. Manuf.* **2015**, *16*, 1085–1093. [[CrossRef](#)]
29. Han, S.; Wang, H.; Tian, Y. Model-free based adaptive nonsingular fast terminal sliding mode control with time-delay estimation for a 12 DOF multi-functional lower limb exoskeleton. *Adv. Eng. Softw.* **2018**, *119*, 38–47. [[CrossRef](#)]
30. Cheng, J.; Zhu, M.; Wang, Y.H.; Yue, H.; Cui, W.X. Cascade construction of working face geological model for intelligent and precise coal mining and its key technologies. *J. Coal* **2019**, *44*, 2285–2295.

Disclaimer/Publisher’s Note: The statements, opinions and data contained in all publications are solely those of the individual author(s) and contributor(s) and not of MDPI and/or the editor(s). MDPI and/or the editor(s) disclaim responsibility for any injury to people or property resulting from any ideas, methods, instructions or products referred to in the content.